NeuroImage: Clinical 19 (2018) 454–465

Contents lists available at ScienceDirect

NeuroImage: Clinical

journal homepage: www.elsevier.com/locate/ynicl

Basal ganglia involvement in *ARX* patients: The reason for *ARX* patients very specific grasping?

Aurore Curie[a,b,c,d,e,*,1], Gaëlle Friocourt[f,g,1], Vincent des Portes[a,b,c], Alice Roy[h], Tatjana Nazir[b], Amandine Brun[b], Anne Cheylus[b], Pascale Marcorelles[i,j], Kalliroi Retzepi[d,e], Nasim Maleki[d,e], Gérald Bussy[b], Yves Paulignan[b], Anne Reboul[b], Danielle Ibarrola[k], Jian Kong[d], Nouchine Hadjikhani[e,l], Annie Laquerrière[m], Randy L. Gollub[d,e]

[a] *Centre de Référence Déficiences Intellectuelles de Causes Rares, Hôpital Femmes Mères Enfants, Hospices Civils de Lyon, Bron, France*
[b] *CNRS UMR5304, Institut des Sciences Cognitives, Bron, France*
[c] *Université Claude Bernard Lyon 1, France*
[d] *Psychiatric Neuroimaging Program, Department of Psychiatry, Massachusetts General Hospital/Harvard Medical School, Boston, MA, USA*
[e] *Athinoula A. Martinos Center for Biomedical Imaging, Massachusetts General Hospital/Harvard Medical School, Boston, MA, USA*
[f] *Inserm UMR1078, Université de Brest, IBSAM, Brest, France; Etablissement Français du Sang (EFS), Bretagne, France*
[g] *CHU Brest, Brest, France*
[h] *Dynamique Du Langage, CNRS UMR 5596, Université de Lyon, Lyon, France*
[i] *Pathology Laboratory, Pole Pathologie-Biologie, Centre Hospitalier Universitaire Brest, Brest, France*
[j] *Laboratory of Neurosciences of Brest, Faculté de Médecine et des Sciences de la Santé, Brest University, Brest, France*
[k] *CERMEP, CNRS UMS3453, Bron, France*
[l] *Gillberg Neuropsychiatric Center, Gothenburg, Sweden*
[m] *Normandie Univ, UNIROUEN, INSERM U1245, Rouen University Hospital, Department of Pathology, F76000 Rouen, France*

ARTICLE INFO

Keywords:
ARX
Human brain development
Intellectual disability
Morphometric MRI
Kinematic
Limb Kinetic Apraxia

ABSTRACT

The *ARX* (*Aristaless Related homeoboX*) gene was identified in 2002 as responsible for XLAG syndrome, a lissencephaly characterized by an almost complete absence of cortical GABAergic interneurons, and for milder forms of X-linked Intellectual Disability (ID) without apparent brain abnormalities. The most frequent mutation found in the *ARX* gene, a duplication of 24 base pairs (c.429_452dup24) in exon 2, results in a recognizable syndrome in which patients present ID without primary motor impairment, but with a very specific upper limb distal motor apraxia associated with a pathognomonic hand-grip, described as developmental Limb Kinetic Apraxia (LKA).

In this study, we first present *ARX* expression during human fetal brain development showing that it is strongly expressed in GABAergic neuronal progenitors during the second and third trimester of pregnancy. We show that although *ARX* expression strongly decreases towards the end of gestation, it is still present after birth in some neurons of the basal ganglia, thalamus and cerebral cortex, suggesting that ARX also plays a role in more mature neuron functioning. Then, using morphometric brain MRI in 13 *ARX* patients carrying c.429_452dup24 mutation and in 13 sex- and age-matched healthy controls, we show that *ARX* patients have a significantly decreased volume of several brain structures including the striatum (and more specifically the caudate nucleus), hippocampus and thalamus as well as decreased precentral gyrus cortical thickness. We observe a significant correlation between caudate nucleus volume reduction and motor impairment severity quantified by kinematic parameter of precision grip.

As basal ganglia are known to regulate sensorimotor processing and are involved in the control of precision

Abbreviations: ARX, Aristaless-Related homeoboX gene (according to the genetic convention, ARX was written in italics when it refers to the gene, in plain-text characters when it refers to the protein, in capital letters when it refers to the human gene, and in lowercase when it refers to the mouse gene); CGE, caudal ganglionic eminence; CP, cortical plate; DS, down syndrome; GE, ganglionic eminences; ICV, intracranial volume; ID, Intellectual Disability; IQ, intelligence quotient; IZ, intermediate zone; LGE, lateral ganglionic eminence; LKA, Limb Kinetic Apraxia; MGE, medial ganglionic eminence; MRI, magnetic resonance imaging; MZ, marginal zone; ROI, region of interest; SGL, subpial granular layer; SVZ, subventricular zone; VZ, ventricular zone; WG, weeks of gestation; XLAG, X-linked lissencephaly with abnormal genitalia

* Corresponding author at: Institut des Sciences Cognitives Marc Jeannerod, CNRS UMR5304, 57 boulevard Pinel, 69500 Bron, France.
E-mail address: aurore.curie@univ-lyon1.fr (A. Curie).
[1] Both authors contributed equally.

https://doi.org/10.1016/j.nicl.2018.04.001
Received 22 November 2017; Received in revised form 5 March 2018; Accepted 1 April 2018
Available online 05 April 2018

gripping, the combined decrease in cortical thickness of primary motor cortex and basal ganglia volume in *ARX* dup24 patients is very likely the anatomical substrate of this developmental form of LKA.

1. Introduction

Mutations in the homeobox transcription factor *ARX* are responsible for a wide spectrum of neurodevelopmental disorders extending from extremely severe neuronal migration defects resulting in three-layered lissencephaly (XLAG syndrome, MIM#300215), to mild forms of Intellectual Disability (ID) without apparent brain abnormalities, but with associated features of dystonia and epilepsy (reviewed in Friocourt and Parnavelas, 2010, Shoubridge et al., 2010, Olivetti and Noebels, 2012). Although Arx expression in mouse has been reported in several developing structures including brain, pancreas, testes, heart, skeletal muscle and liver (Miura et al., 1997; Bienvenu et al., 2002; Kitamura et al., 2002; Collombat et al., 2003; Biressi et al., 2008), the most striking consequences of *Arx* loss of function affect brain and testes, both in mice and humans (Bonneau et al., 2002; Kitamura et al., 2002; Colombo et al., 2007; Marcorelles et al., 2010). In the developing and adult rodent brain, Arx expression in telencephalic structures, particularly in populations of GABA-containing neurons, has been extensively described (Colombo et al., 2004; Poirier et al., 2004; Cobos et al., 2005; Friocourt et al., 2006; Friocourt et al., 2008). Studies of the effects of *ARX* loss of function either in humans or in in mutant mice have shown that this gene plays multiple roles during development, most importantly in the generation and migration of GABAergic interneurons (see for review Friocourt and Parnavelas, 2010), leading, when mutated, to a disorder of interneurons, called “interneuronopathy” (Kato and Dobyns, 2005; Price et al., 2009). More recently, Arx has been shown to be also involved in the development of excitatory neurons (Friocourt et al., 2008; Beguin et al., 2013; Colasante et al., 2015; Simonet et al., 2015) through its expression in cortical progenitors, thus explaining the microcephaly phenotype observed in knock-out mice and human XLAG patients (Bonneau et al., 2002; Kitamura et al., 2002).

Although the general steps of brain development are conserved between human and rodents, there are some differences, in particular concerning the number and complexity of GABAergic interneurons that greatly increase relatively to glutamatergic neurons during mammalian and particularly primate evolution (Rakic, 2009). Since no detailed description of ARX expression in human brain has ever been performed, we decided to investigate human ARX expression using immunohistochemistry at different fetal stages as well as in an adult case. Then, to further investigate the role of ARX in brain development and function, we focused on the *in vivo* phenotypic characterization of the most frequent mutation found in this gene, *i.e.* a duplication of 24 base pairs (c.429_452dup24, noted dup24) leading to a polyalanine tract expansion, which is thought to result in a decreased amount of ARX protein (Lee et al., 2014) and/or the deregulation of a subset of ARX target genes (Friocourt and Dubos, unpublished data). This mutation results in a relatively mild phenotype that can be more deeply explored than very severe phenotypes such as XLAG syndrome, which are most often lethal shortly after birth. By clinically reviewing all affected patients identified in France over a five-year period (*i.e.* 27 patients from 12 different families), we recently described a very specific phenotype associated with this mutation (Curie et al., 2014). All *ARX* patients exhibited ID with no primary motor impairment, but with a very specific upper limb distal motor apraxia associated with a pathognomonic hand-grip. A spectrum of severity level is observed ranging from the milder form, exhibiting atypical handling and/or articulation impairment, to the most severe form, the so-called Partington syndrome, with major hand dystonia and/or oro-lingual apraxia. The particular “reach and grip” impairment was further characterized by kinematic analysis, and consisted of loss of preference for the index finger when gripping an object, major impairment of fourth finger deftness and lack of pronation movements. This lack of distal movement coordination was associated with the loss of independent digital dexterity, similarly to the distortion of individual finger movements and posture observed in Limb Kinetic Apraxia (LKA). These findings led us to suggest that the *ARX* dup24 mutation may be a developmental model for LKA (Curie et al., 2014).

In the present study, we performed for the first time a study of ARX expression at the protein level both during fetal human development and in an adult brain, as well as MRI morphometric analyses (1.5 T) on 13 *ARX* dup24 patients compared to 13 sex- and age-matched healthy controls using FreeSurfer software, a very powerful tool both for surface, in particular cortical thickness measurement at each point across the cortical mantle, and volumetric analyses (Dale et al., 1999; Fischl et al., 1999; Fischl and Dale, 2000; Fischl et al., 2001; Han et al., 2006;

Table 1
Semi-quantitative analysis of *ARX* expression in the developing central nervous system.

		13–18 WG	22–28 WG	30–36 WG	40 WG	Adult
Telencephalon	Marginal zone/Layer I	+ + +	+ + +	+ +	+ +	+
	Cortical plate	+ + +	+ + +	+ +	+ +	+ +
	Intermediate zone	+ + +	+ + +	+	+	0
	ventricular and subventricular zones	+ + + +	+ + +	+	NA	NA
	Hippocampus	+ + +	+ + +	NA	NA	NA
	Ganglionic eminences	+ + + +	+ + + +	+ + +	+	NA
	Caudate nucleus	+ + +	+ + +	+ +	+	+
	Putamen	+ + +	+ +	+	+	NA
	Globus pallidus	+ + +	+ +	+	+	NA
	Substantia innominate, Basal nucleus of Meynert	+ + +	+ +	+	+	NA
Diencephalon	Preoptic area	+ + +	+ +	NA	NA	NA
	Medial and posterior hypothalamus	+ + +	+ + +	+ +	NA	NA
	Thalamic nuclei	+ + +	+ + +	+ +	NA	NA
	Amygdala	+ + +	+ + +	NA	NA	NA
Cerebellum		0	0	0	0	0

+ + + +: most of the cells of the structure are strongly labelled.
+ + +: a fraction of the cells of the structure is strongly labelled.
+ +: some cells are labelled.
+: very few cells are labelled.
0: no cells are labelled.
NA: not available.

Segonne et al., 2007). The goal of the present study was to find a potential neuro-anatomical distinctive pattern associated with this mutation of *ARX*, a gene highly expressed during neurodevelopment, that could help in explaining the specific developmental LKA observed in *ARX* dup24 patients.

2. Material and methods

2.1. Neuropathological studies

2.1.1. Patient selection

Thirteen fetal brains ranging from 13 to 40 weeks of gestation (WG) along with an adult case were selected (Table 1). None of the studied cases displayed any particular medical familial history of neurological disease and all brains were macroscopically and microscopically free of detectable abnormalities. The brains used in this study belong to the collection which has been declared to the French Ministry of Health (collection number DC-2015-2468, cession number AC-2015-2467). This collection is located in the Pathology Laboratory, Rouen University hospital. For all selected cases, parents had given their consent for neuropathological studies of the foetuses following autopsy performed in agreement with the local ethic committee and in accordance with the French law. In each case, a complete autopsy had been performed. Cases who were suspected of central nervous system anomalies or who had been suspected of dying from neurologic causes were systematically excluded. Main causes of death were spontaneous death in single or twin pregnancies after premature rupture of membranes or chorioamnionitis (Supplementary Table 1).

Brain growth of fetal and neonatal cases was evaluated according to the criteria of (Guihard-Costa and Larroche, 1990). Macroscopic evaluation of brain maturation, in particular gyration, was performed according to the atlas of Feess-Higgins and Larroche (Feess-Higgins and Larroche, 1987). After fixation into a zinc-10% formalin buffer solution for one month, 7 µm paraffin embedded sections were stained using Haematoxylin-eosin and Cresyl Violet, which made it possible to confirm the absence of cerebral lesions. The morphology of all different brain structures studied was consistent with the age of the patients. Microscopic analysis of the different neuroanatomical structures was performed according to Bayer and Altman's atlas of human central nervous system development (Bayer and Altman, 2004).

2.1.2. Immunohistochemical procedures

Five micrometer coronal sections were cut from formalin-fixed paraffin-embedded blocks, mounted on coated slides (Silanized Slides S 3003 Dako, Trappes, France) and dried overnight in a convection oven (37 °C). Sections were deparaffined in three baths of xylene and rehydrated in a series of ethanol solutions. Induced epitope retrieval was performed by immersion in a citrate buffer solution pH 6 at 95–99 °C for 1 h. Slides were then rinsed in distilled water and left to cool down. Different pre-treatments and dilutions were tested to determine the optimal dilution (1/500) for the polyclonal anti-ARX antibody (Poirier et al., 2004). Incubations were performed for 1 h at room temperature using the TECHMATE 500 system (Dakopatts, Trappes, France). After incubation, slides were processed by Labelled Streptavidin Biotin Method (LSAB) detection kit (Dakopatts). Peroxidase was visualized either using 3-3′ diaminobenzidine or amino-ethyl-carbazole. A negative control was obtained by omission of the primary antibody. The specificity of ARX labelling was further confirmed by the absence of staining in the cerebellum, which does not express ARX as previously described in mice (Poirier et al., 2004). As ARX is a transcription factor primarily expressed in neuron nuclei, immunoreactivities appeared as brown dots within nuclei compared to blue negative-nuclei counterstained with Haematoxylin.

2.2. Neuroimaging analyses

2.2.1. Study participants: ARX patients and age- and sex-matched healthy controls

ARX patients were recruited through their primary care doctor or the specialist who asked for molecular testing. Most of the patients are followed in the National Reference Centre for Rare Diseases with Intellectual Disability (Lyon, France). After having clearly explained the goals of this study, all patients and their guardians gave their written informed consent in accordance with the Ethical Committee protocols of French Public Hospitals. Data were collected at CERMEP (Centre d'Etude et de Recherche Multimodal Et Pluridisciplinaire) in Lyon. Molecular screening for *ARX* gene was performed in laboratories from a French network dedicated to neurogenetic testing as previously described (Poirier et al., 2006). Age- and sex-matched healthy controls were recruited through local advertisements. Adult healthy control participants and the parents of each child included in the study signed an informed consent before the study procedure started.

Thirteen *ARX* patients and 13 age- and sex-matched healthy controls were included in the study and completed brain MRI. All *ARX* patients exhibited the same mutation in the *ARX* gene, the 24 base pair duplication (c.429_452dup24) in exon 2 resulting in a polyalanine tract expansion responsible for an insertion of 8 alanine residues in the ARX protein. Subjects having any contraindications to MRI scanning (such as cardiac pacemaker, metal clips or implants, osteosynthesis material and claustrophobia) or non-correctible visual impairment were systematically excluded. An additional exclusion criterion for healthy controls was having a history of neurological or psychiatric disorder. The mean age was 20.3 years [6.3–40.3] for the *ARX* patient group and 20.6 years [7.5–42.3] for the age- and sex-matched healthy control group. The mean Head Circumference (HC) was −0.2SD [−1.5 to +1] and + 0.8SD [−1 to +2] in the *ARX* and age- and sex-matched healthy control group respectively. All *ARX* patients had an IQ below 70. The mean adaptive global score (Vineland Adaptive Behavior Scale) in the *ARX* patient group was 44.5 [30–59].

In order to avoid major age-related variations in brain size and myelination, we did not include for volumetric and surface analyses, patients under the age of 10 that led us to exclude the two youngest *ARX* patients aged 6 years 4 months and 9 years 3 months old respectively and their age- and sex-matched healthy controls.

2.2.2. Kinematic measurements

A kinematic study of a grasping movement was performed in all participants, whose results have previously been published (Curie et al., 2014). The task consisted of reaching, grasping and lifting a plastic parallelepiped block (50 * 30 * 15 mm) from a specific starting point. The kinematic parameter which was the most impaired in *ARX* patients was the time to Maximum Grip Aperture (MGA) also called MGA latency when grasping the object with the thumb-annular pinch at −56° (Curie et al., 2014). We thus considered that this kinematic parameter was a good indicator of the motor impairment severity in *ARX* patients.

2.2.3. Procedures and MRI acquisition

Due to the unique challenges resulting from the environment of the fMRI scanner in ID patients, special attention was given to spend adequate time acclimating the patients to each aspect of the fMRI scan session experience using a mock scanner. Reassurance was necessary at each step such as helping them to feel comfortable lying on a moving bed, adjusting to the sensations of having their head within the head coil, being in a noisy environment (scanner) without being afraid, and getting used to looking into a mirror to watch a movie during data acquisition. They first watched a family member or staff member lying down in a mock scanner, to help them understand that it was painless. Then *ARX* patients were trained in a mock MRI scanner not to move. This training also decreased their anxiety. One to three sessions in the mock scanner were necessary per patient. The actual MRI session then

followed. During the morphometric data acquisition (3DT1) all participants were watching a movie.

Image acquisition was performed on a 1.5 T Siemens scanner (CERMEP, Lyon). High resolution (1 × 1 × 1 mm) structural imaging with 3D T1-weighted Fast-Spoiled Gradient Recalled (FSPGR) sequence (TR/TE/TI = 1970/3.93/1100 ms, FOV = 256 × 256 mm) was obtained for each patient and age-matched healthy control. In addition, a T2 sequence was performed (51 axial slices, FOV = 220 mm, voxel size: 0.9 × 0.9 × 2.5 mm, TR/TE = 7740 /96 ms).

2.2.4. MRI data analysis

MRI images were clinically reviewed by two paediatric neurologists from the National Reference Centre for Rare Diseases with Intellectual Disability (Lyon, France). The vermian height was determined on the T1-weighted sagittal medial view of each individual. The normality of the vermian height distribution was checked using a Shapiro-Wilk normality test. A one-way ANOVA test was applied to compare differences between groups.

MRI data were processed on a Linux workstation (MGH Martinos

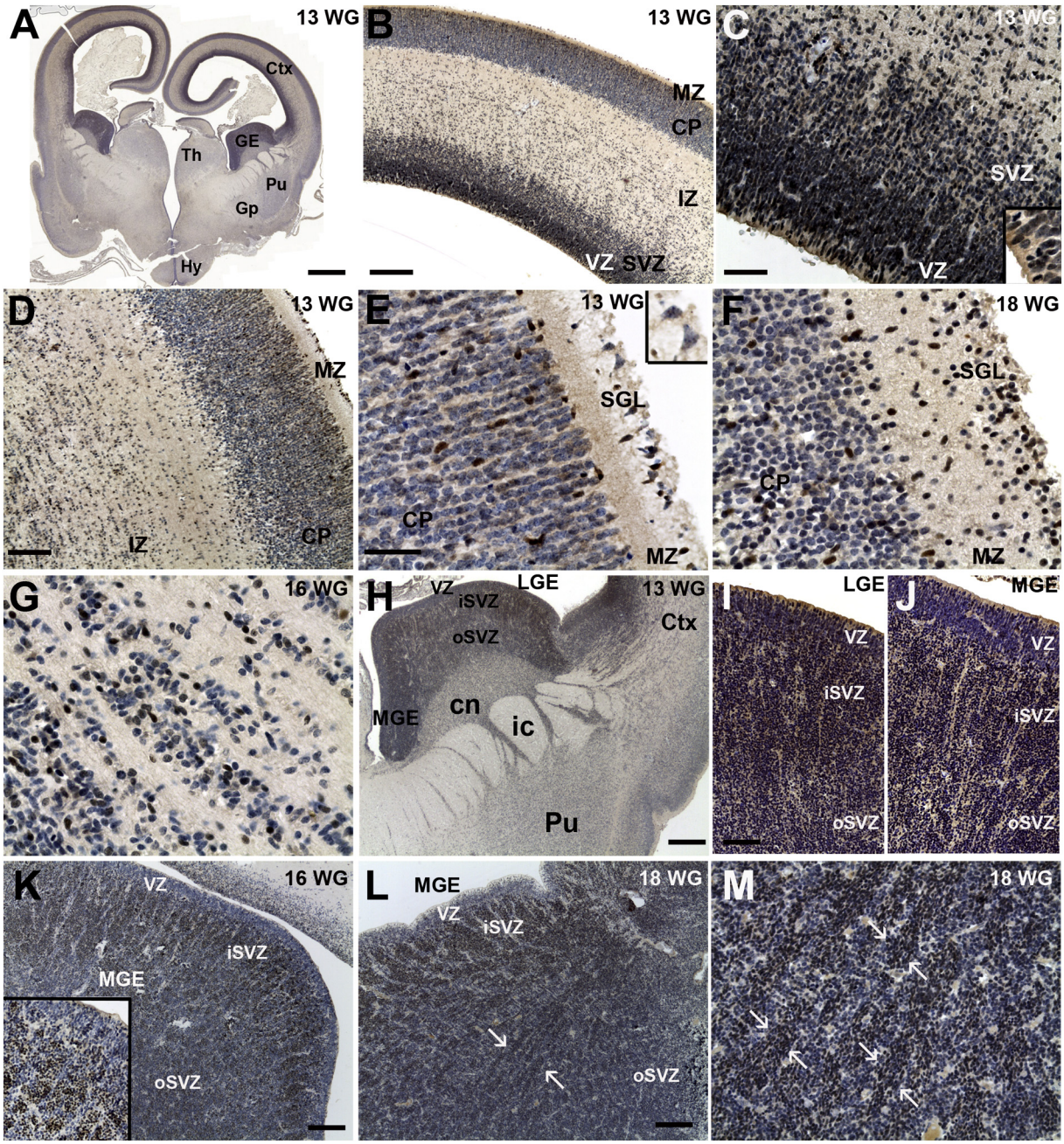

Fig. 1. ARX expression in the developing cortex and ganglionic eminences. At 13 weeks of gestation (WG), the dorsal telencephalon was very strongly labelled (A–B), in particular neuronal progenitors of the ventricular (VZ) and subventricular zone (SVZ), in which the vast majority of cells were ARX-positive (B–C), including dividing cells as observed with H&E and Cresyl Violet staining of the nuclei (inset, C). In the intermediate zone (IZ), approximately 40 to 50% of the cells were ARX-positive (D). In the MZ, several nuclei positive for ARX had an orientation suggestive of inward migration towards the upper part of the cortical plate (CP) (E–F). Cajal-Retzius cells were negative (E, inset). In the SVZ/IZ, several ARX-labelled cells were tangentially orientated (G). Several labelled cells were also detected in the putamen (Pu) and caudate nucleus (cn) (H). In the lateral ganglionic eminence (LGE), ARX-expressing cells were present in the ventricular zone (VZ) and inner (iSVZ) and outer subventricular zone (oSVZ) (I) whereas only rare ARX-expressing cells were present in the VZ of the medial ganglionic eminence (MGE) (J). Streams of ARX-positive post-mitotic neurons tangentially migrating around clusters of non-labelled progenitors were detected in the iSVZ (K) and oSVZ (L–M) of the MGE. SGL: subpial granular layer, Gp: globus pallidus, Th: thalamus, Hy: hypothalamus. Scale bars: A, 2 mm, B, H, 500 µm, C, 100 µm, D, I-L, 200 µm, E–G, 50 µm.

Center, Boston, USA), using FreeSurfer software version 5.1 (http://surfer.nmr.mgh.harvard.edu), to reconstruct the cortical surface. FreeSurfer uses a series of computationally intensive steps on the T1-weighted structural volumes to estimate the grey/white interface (Dale et al., 1999; Fischl et al., 1999; Fischl et al., 2002). These steps include motion correction and averaging, computing Talairach transforms, intensity normalization, skull stripping, tessellation of the grey matter/white matter boundary, automated topology correction, automatic volume labelling and white matter segmentation. The accuracy of the reconstruction of pial and white matter surfaces and the subcortical segmentation were manually checked for every subject, by displaying each segmentation result (aseg.mgz file) in tkmedit. Any inaccuracies in the reconstruction of white and pial surfaces or in the subcortical segmentation of individual subject were manually corrected in each case before calculating the cortical thickness. Cortical thickness measurements were computed as the distance between the pial and white matter surfaces at each point across the cortical cortex surface. Data were then aligned according to cortical folding (Dale et al., 1999) and smoothed on the surface tessellation, using an iterative nearest neighbour procedure. Smoothing was restricted to the cortical surface, thus avoiding the averaging of data across sulci or outside the grey matter (Dale et al., 1999). This method has the advantage of matching morphologically homologous cortical areas based on the main gyri/sulci patterns with minimal metric distortion.

Group analyses were performed by resampling each subject's data to the FreeSurfer average atlas. Cortical thickness maps were smoothed using a Gaussian kernel with a full width half maximum of 10 mm. Vertex-wise analyses of cortical thickness were performed with FreeSurfer. A general linear model was used to compare cortical thickness between groups with one discrete factor with two classes: *ARX* patients and age-matched healthy controls. The statistical threshold was set at $p < 0.05$, cluster-based corrected for multiple comparisons using Monte-Carlo simulation. Analyses of the relationships between cortical thickness measurements in *ARX* patients and neuropsychological data (Vineland Adaptive Behavior Scale) were performed by means of linear regression within FreeSurfer.

The automated procedure for labelling different brain structures and getting their volumetric measurements is described in detail elsewhere (Fischl et al., 2002). This procedure assigns a neuroanatomical label to each voxel in an MRI volume based on probabilistic information automatically estimated from a manually labelled training set, including both grey and white matter. Automated segmentation and cortical parcellation with FreeSurfer has been shown to be robust and reliable in adults and children over the age of 5. It has also been performed in patient populations with known brain abnormalities. Statistical analyses of brain volumes were performed using R software (http://www.r-project.org). The normality of data distribution was first checked using the Shapiro and Wilk normality test. Then a between group analysis (*ARX* patients and age-matched healthy controls) was performed using an ANOVA. The statistical threshold was set at $p < 0.05$, Bonferroni corrected. As we were expecting differences in brain size between *ARX* patients and healthy controls, we added an additional analysis on normalized brain volume for each Region Of Interest (ROI), by dividing each ROI volume of each subject by the intracranial volume corresponding to each subject (O'Brien et al., 2011). Correlation analyses between ROI volumes and kinematic measurement (MGA latency) within a given participant group were performed using the Pearson correlation coefficient. We used Slicer 3.4 (http:www.slicer.org) to build a 3D model of the basal ganglia in ARX and age- and sex-matched healthy controls.

3. Results

3.1. ARX is strongly expressed in tangentially migrating progenitors of GABAergic neurons

In the developing human brain, ARX was found mainly expressed in regions rich in GABAergic neurons such as the hippocampus (dentate gyrus), the amygdaloid complex and the thalamic reticular nucleus. ARX was also found particularly enriched in the ganglionic eminences (GE) that are the main source of GABAergic cortical interneurons and of striatal neurons (Marin et al., 2000; Parnavelas, 2000). The globus pallidus and other basal ganglia related nuclei (substantia innominata and basal nucleus of Meynert) also contained numerous ARX-positive neurons. In addition, ARX was found particularly enriched in non-radially migrating neurons (Corbin et al., 2001), such as cortical interneurons migrating from the GE, neurons of the rostral migratory stream migrating from the subventricular zone of the lateral ventricle to the olfactory bulb, and neurons of the gangliothalamic body migrating from the GE to the dorsal thalamus. Unlike cortical projection progenitors that migrate along radial-glial cell processes, these neurons rely on neurophilic interactions and migrate closely together (called chain-migration) following extracellular cues such as semaphorins to reach their final position in the brain (Corbin et al., 2001). Towards the end of gestation, both the number of labelled cells and the level of ARX expression slowly decreased and at birth, it was only expressed in a fraction of cells in the same structures (Table 1). In the adult brain, ARX was still strongly expressed in neurons of layers II and IV of the cerebral cortex as previously observed for cortical interneurons (Xu et al., 2011) and in the caudate nucleus, suggesting a role not only in neuronal migration and development but also in more mature neurons.

3.1.1. ARX expression in the developing cerebral cortex

During the second trimester of gestation, the cerebral cortex was very strongly labelled, especially the ventricular (VZ) and subventricular zone (SVZ) (Fig. 1A–C), suggesting a role of ARX in cortical neuronal progenitors, similarly to what has been described in mouse (Friocourt et al., 2008; Colasante et al., 2015; Simonet et al., 2015). In the marginal zone (MZ), several cells were positive in the transient subpial granular layer (SGL) (Fig. 1D–F, see Supplementary data). In the SVZ, as well as in the cortical intermediate zone (IZ) and subplate, many strongly positive tangentially-orientated nuclei were visible, probably corresponding to migrating interneurons coming from the medial ganglionic eminence (MGE) (Fig. 1D, G). At all early stages, strongly labelled cells were scattered in all the developing hippocampus, including Ammon's horn and the presumptive dentate gyrus (data not shown).

3.1.2. ARX expression in the ganglionic eminence (GE) and basal ganglia

GE consists of transitory brain structures that are divided anatomically into three parts, the medial (MGE), lateral (LGE) and caudal ganglionic eminence (CGE). The MGE gives rise to pallidal projection neurons and to cortical and striatal interneurons (Marin et al., 2000; Nobrega-Pereira et al., 2010), the LGE, which is dorsal to the MGE, produces striatal projection neurons, olfactory bulb interneurons and possibly cortical interneurons and finally, the CGE generates subtypes of interneurons that are destined for cortex, hippocampus, amygdala and other limbic system nuclei, as well as caudal striatal and pallidal neurons (Clowry, 2015). At all fetal stages, the GE were very strongly labelled (Fig. 1H–M), especially intermediate progenitors of the inner subventricular zone (iSVZ) (Fig. 1H–K, see Supplementary data for a more detailed description). Interestingly, although most of the neuronal stem cells composing the VZ expressed ARX in the LGE, ARX was only detected in rare cells in the VZ of the MGE (Fig. 1I–J), suggesting that neuronal stem cells have distinct identities in the MGE and LGE.

ARX was also strongly expressed in migratory streams of neurons leaving the LGE and MGE (see Supplementary data for a more detailed

description of ARX expression in GE). Accordingly, several ARX-positive cells migrating from the adjacent LGE were detected at the boundary between the caudate nucleus and the LGE. Similarly, streams of ARX-expressing cells were also detected in the striatal bridges connecting caudate nucleus and putamen (Fig. 2A–C). At 32 WG, ARX-expressing cells were also detected in the nucleus accumbens which is a component of the striatum, and also a part of the limbic system (Fig. 2D).

3.1.3. ARX immunoreactivity in the diencephalon and basal telencephalic structures

In the developing diencephalon, ARX was absent from the VZ of the third ventricle, but strongly expressed in scattered cells of the developing thalamus (Fig. 2E), especially in the periventricular complex and the reticular nucleus, and to a lesser extent, in dorsal and ventral nuclei of the anterior complex. The ventral thalamus and hypothalamus also displayed several ARX-positive cells in close proximity to the ventricle (Fig. 2F–G). Between 22 and 32 WG, ARX expression was also identified in the gangliothalamic body (Fig. 2H), a voluminous stream of migrating bipolar neurons only observed in humans and not found in any other species, and regarded as a corridor through which neurons migrate from the GE to the dorsal thalamus (Letinic and Kostovic, 1997; Letinic and Rakic, 2001).

Overall, these data suggest that ARX is particularly important for the generation and migration of GABAergic cells in the cortical plate, basal ganglia and basal telencephalic structures. After the development of these structures is completed, ARX expression is strongly decreased but is still maintained in some cells of the same structures (Table 1), suggesting a role of ARX, not only during development but also in more mature neurons.

3.2. Clinical MRI analysis in ARX patients and age- and sex-matched healthy controls

No major brain malformation was found in the 13 *ARX* dup24 patients or the 13 age- and sex-matched healthy controls. Non-specific MRI features were observed in six *ARX* patients. Two *ARX* patients had a mild ventriculomegaly (lateral ventricles were 11 and 12 mm wide respectively), two had ventricular asymmetry without dilatation, one had postero-superior vermis atrophy (lobules VI and VII) associated with an enlargement of the horizontal hemispherical cerebellar fissure and one *ARX* patient had a retro-cerebellar arachnoid cyst. Dilated Virchow Robin (VR) spaces were found in all *ARX* patients along the lenticulo-striate arteries, but 8 aged-matched healthy controls also had enlarged VR spaces, a sign which is not specific. No significant difference in vermis height was found between *ARX* patients and healthy

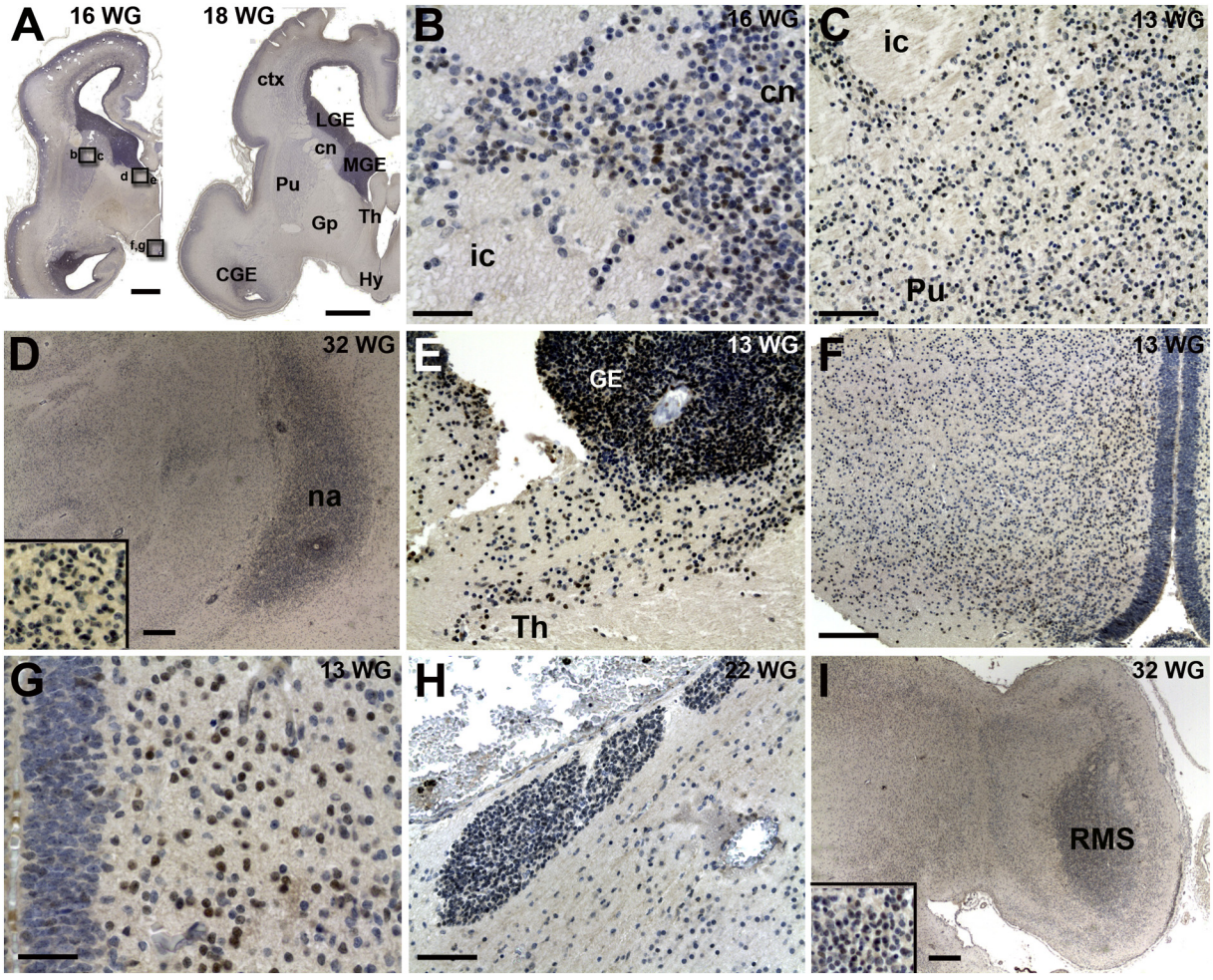

Fig. 2. ARX expression in the developing subpallium. ARX expression at 16 and 18 WG (A). Outlined boxed areas are magnified in the following panels at different stages. ARX antibody labelled several cells in the caudate nucleus (cn) (B) and cells migrating towards the putamen (Pu) through the internal capsule (C). At 32 WG, several ARX-expressing cells were detected in the nucleus accumbens (na) (D). Scattered cells expressing ARX were also detected in neurons migrating from the GE towards the thalamus (Th) (E) through the gangliothalamic body (H) and in the developing hypothalamus (Hy) (F, G). At 32 WG, several ARX-expressing cells were detected in the rostral migratory stream (RMS) in the olfactory tubercle (I) ctx: cortex, LGE, MGE, CGE: lateral, medial and caudal ganglionic eminence. Scale bars: A, 5 mm, B, G, 50 µm, C, E, H, 100 µm, F, 200 µm, D, I, 1 mm.

controls (mean vermis height of 47.8 mm (SD 3.3) and 47.2 mm (SD 2.5) in *ARX* patients and age- and sex-matched healthy controls respectively).

3.3. Brain volumetric analyses in ARX patients and age- and sex-matched healthy controls

Regarding global brain volumes, no significant group effect was found on intracranial volume, white matter (WM), cerebellar, corpus callosum and lateral ventricle volume when comparing *ARX* dup24 patients and age- and sex-matched healthy controls (Table 2). Even after normalization by intracranial volume, *ARX* patients had similar cerebellar volume compared to age- and sex-matched healthy controls ($F(1,20) = 0.3$, $p = 0.6$), which is consistent with the absence of *ARX* expression in the developing and adult cerebellum that we observed here and that was previously reported in rodents. However, a significant group effect was found for the volume of the caudate nuclei, as well as of the hippocampi (Table 2). More precisely, *ARX* dup24 patients had a significantly decreased striatal volume, mainly involving the caudate nuclei, compared to age-and sex-matched healthy controls (Fig. 3A and B). After normalization by intracranial volume, the group effect was still significant on caudate nuclei ($F(1,20) = 7.5$, $p = 0.01$). Moreover, we found a significant correlation ($r^2 = 0.46$, $p = 0.001$, Fig. 3C) between the caudate nucleus volume and the degree of motor impairment quantified by the kinematic parameter which was the most impaired in *ARX* patients (Curie et al., 2014): the smaller the caudate nucleus volume was, the more impaired the kinematic parameter was.

We also observed a significant decrease of the hippocampal volume in *ARX* patients compared to age- and sex-matched healthy controls. We observed a decreased volume of thalamic and sub-thalamic nuclei in *ARX* patients compared to age- and sex-matched healthy controls, but this did not reach significance (it was only a trend, likely by lack of power in this study on a rare disease, Table 2). We found no correlation between the volume of thalamic and sub-thalamic nuclei and the severity of motor impairment ($r^2 = 0.09$, $p = 0.82$ and $r^2 = 0.44$, $p = 0.24$ for thalamic and sub-thalamic nuclei respectively).

Interestingly, we also found a slight but significant decrease of the hemispheric grey matter volumes in *ARX* dup24 patients (Table 2), suggesting that they may have a small global decreased number of neurons, which is consistent with the expression of ARX in both glutamatergic and GABAergic neuronal progenitors and the observed microcephaly in both mouse and human patients with severe loss-of-function mutations of *ARX* (Bonneau et al., 2002; Kitamura et al., 2002).

3.4. Cortical thickness analysis in ARX patients and age- and sex-matched healthy controls

We observed that the precentral gyrus, a part of the primary motor cortex, was significantly and bilaterally thinner in the *ARX* patient group compared with the age- and sex-matched healthy control group (Table 3, Fig. 4). In addition, the correlation between precentral gyrus cortical thickness and caudate volume was significant ($r^2 = 0.57$, $p = 0.005$ and $r^2 = 0.50$, $p = 0.019$ on the right and left hemisphere respectively). More precisely, the smaller the caudate nucleus was, the thinner the precentral cortical thickness was. This suggests that together with the decreased volume of the caudate nuclei, these morphometric findings very likely explain the specific motor phenotype observed in *ARX* dup24 patients.

A significant association was also found within the *ARX* patient group between cortical thinning and the Vineland Adaptive Behavior scale in prefrontal cortex bilaterally: the thinner the prefrontal cortex was, the lower the Vineland scale was (Fig. 5), suggesting that prefrontal cortex decreased thickness may be related to the ID observed in these patients. Anatomical studies in primates have shown that the caudate and anterior putamen receive afferents from dorsal lateral prefrontal regions and pre-SMA (Vaillancourt et al., 2007). We thus also analyzed the correlation between prefrontal cortical thickness and caudate volume, which was significant ($r^2 = 0.68$, $p = 0.0005$ and $r^2 = 0.58$, $p = 0.004$ on left and right hemisphere respectively). More precisely, the thinner the prefrontal cortical thickness was, the smaller the caudate was.

4. Discussion

In this study, we report for the first time ARX expression in the human developing and adult brain and describe a specific neuroanatomical pattern associated to *ARX* dup24 that very likely represents the substrate of the peculiar developmental Limb Kinetic Apraxia (LKA) observed in these patients.

4.1. ARX expression in progenitors of GABAergic neurons

Although there are many differences in brain development between

Table 2
Brain volumetric analyses in *ARX* patients and age- and sex-matched healthy controls.

Brain Region	Mean Volumes		Standard deviation volumes		Group effect	
	HC	*ARX*	HC	*ARX*	*F*	*p*
Global Volumes						
Total Intracranial Volume	1,711,658.5	1,638,059.2	110,728.3	137,066,7	1.9	NS
GM Volume	801,400.7	735,045.3	74,387.1	62,258.6	5.1	0.035
WM Volume	548,929.9	524,496.9	41,439	70,714.2	0.98	NS
Brain Stem	23,319.2	22,224.9	2774.6	1783.7	1.2	NS
Corpus Callosum Volume	3365.4	3465.9	353.1	453.1	0.3	NS
Lateral Ventricule Volume	10,334.4	18,038.6	3957.1	12,903.1	3.6	NS
Cerebellum						
Global cerebellum Volume	158,348.8	153,572.3	18,648	7433	0.6	NS
WM Volume	30,097.5	31,240.3	5764.3	3191.7	0.3	NS
GM Volume	128,251.4	122,332	13,856.9	8164.2	1.5	NS
Sub-cortical Structures						
Caudate Volume	8333.8	6994.5	756.3	953.7	13.3	0.0016
Putamen Volume	12,783.1	11,987.5	1436	1143.2	2.1	NS
Pallidum Volume	3900.4	3618.7	505.9	663.3	1.25	NS
Thalami Volume	16,118.3	14,985.6	1699.9	1210.2	3.2	0.08
Sub-Thalami Volume	8597.1	7877	1001.0	720.5	3.75	0.06
Hippocampus	9435.7	8592.9	534.1	775.5	8.8	0.007
Amygdala	3679.5	3346.8	477.7	368.5	3.3	NS

GM: Grey Matter, WM: White Matter, NS: Not Significant.

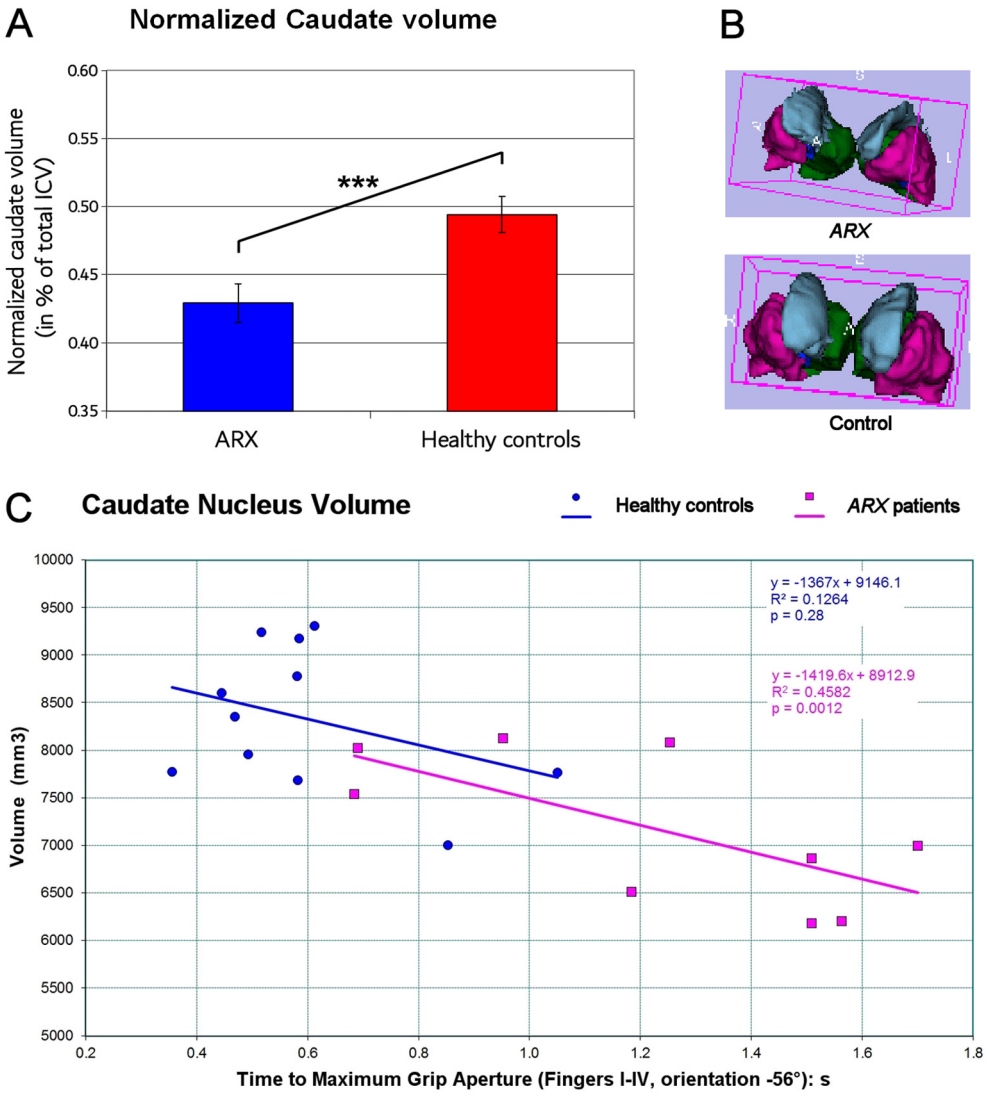

Fig. 3. Basal ganglia volume analysis in *ARX* patients and age- and sex-matched healthy controls. A: Normalized caudate volume in *ARX* patients and age- and sex-matched healthy control subjects showing significantly decreased volume in *ARX* patients (***: $p < 0.005$); B: 3D modelization of the basal ganglia clearly shows the decreased volume of the caudate nucleus (light blue) in *ARX* patients compared to age- and sex-matched healthy controls; C: Correlation between caudate nucleus volume and the kinematic parameter. (For interpretation of the references to color in this figure legend, the reader is referred to the web version of this article.)

Table 3
Areas of significant cortical thinning in *ARX* dup24 patients compared with age-matched healthy controls.

Cluster size	Brain region	Hemisphere	MNI coordinates			*p* value (CWP)
(# Vertex)			*x*	*y*	*z*	
3225	Precentral Gyrus	Left	−18.3	−22.5	71.4	0.0167
3035	Precentral Gyrus	Right	47.3	2.7	30.8	0.0106

MNI: Montréal Neurological Institute.
CWP: ClusterWise *p*-value.

rodents and humans, especially regarding the number and complexity of interneurons, we observed that ARX pattern of expression in human fetal brain is approximately similar and concordant with what has been previously reported in rodents (Miura et al., 1997; Kitamura et al., 2002; Colombo et al., 2004; Poirier et al., 2004; Cobos et al., 2005; Friocourt et al., 2006; Friocourt et al., 2008). We found that during development, the most strongly labelled structures were the germinal

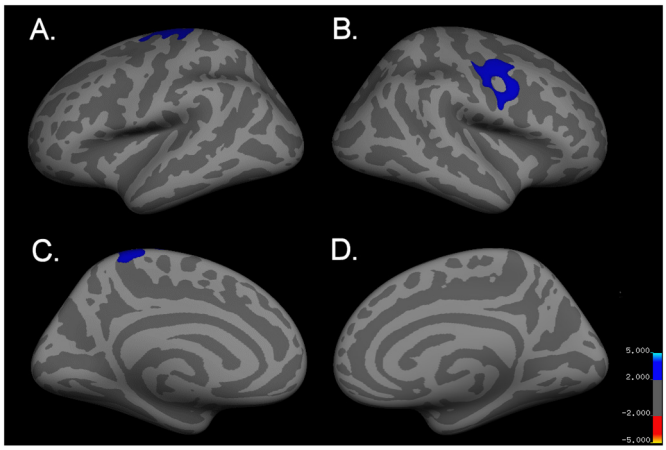

Fig. 4. Mean thickness difference significance maps. Lateral and medial inflated views of the brain showing areas presenting cortical thinning in the ARX patient group compared with age-matched healthy control group (A: left lateral inflated view, B: right lateral inflated view, C: left medial inflated view, D: right medial inflated view).

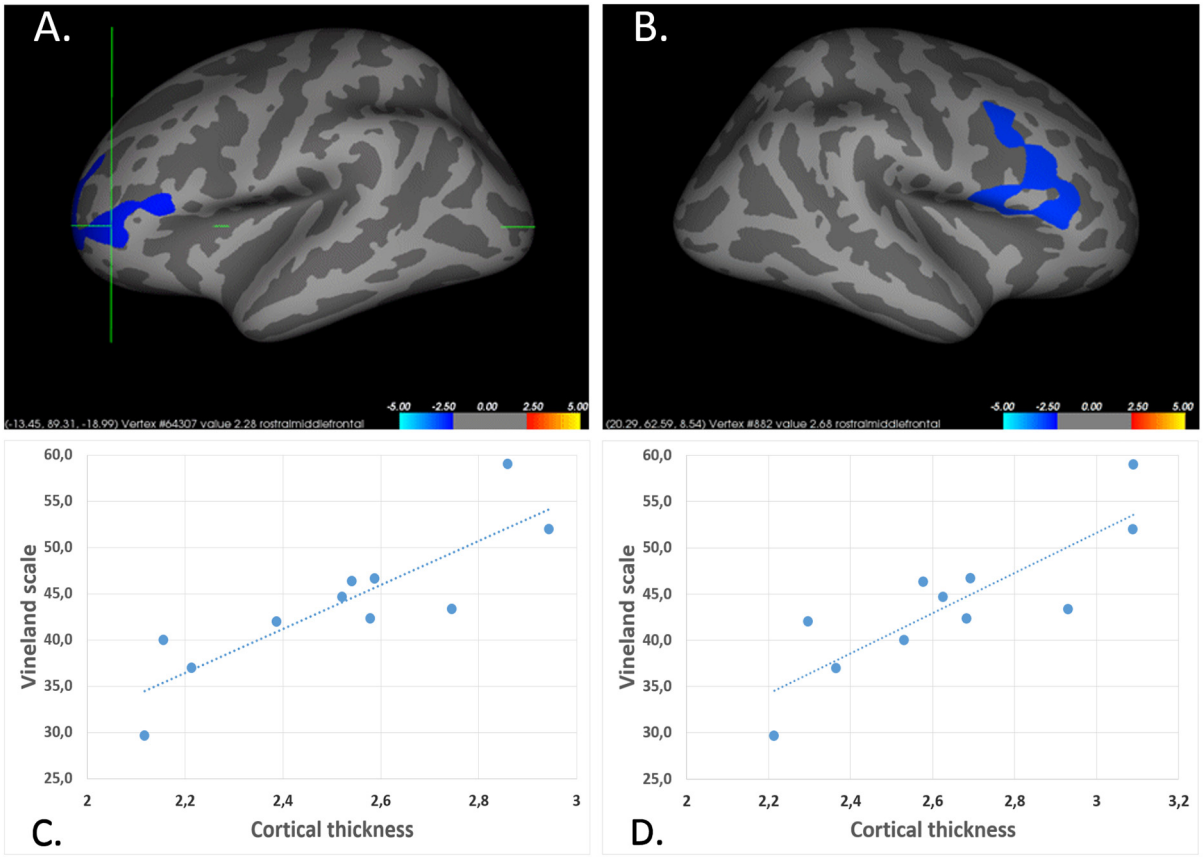

Fig. 5. Correlation between cortical thickness and the Vineland Adaptive Behavior scale. A and B: Cortical brain maps showing the significant association between cortical thinning and the Vineland Adaptive Behavior scale within the *ARX* patient group; C: Correlation between the cortical thickness of the Left prefrontal region and the Vineland scale ($r^2 = 0.86$, $p = 0.0006$); D: Correlation between the cortical thickness of the Right prefrontal region and the Vineland scale ($r^2 = 0.85$, $p = 0.0009$).

zone of dorsal telencephalon, the cortical plate and the GE (Table 1). In addition to the caudate nucleus and putamen, several strongly ARX-positive cells were also identified in the nucleus accumbens, in the pallidum and related nuclei such as substantia innominata and basal nucleus of Meynert. All these data suggest that similarly to rodents, the GE contributes to GABAergic neuron production for the striatum and the limbic system (Marin et al., 2000; Nobrega-Pereira et al., 2010; Pombero et al., 2011; Hansen et al., 2013) and that ARX is required for the development of these structures. In addition, ARX was found to be strongly expressed in many cortical neurons using a non-radial mode of migration based on neurophilic interactions, confirming that ARX may play a role in this type of migration as previously suggested by experiments in which Arx overexpression in cortical progenitors was sufficient to induce tangential dispersion of immature projection neurons in mouse cerebral cortex (Friocourt et al., 2008; Friocourt and Parnavelas, 2010).

In conclusion, we observed the strongest expression of *ARX* between 12 and 22 GW. Then during the third trimester of gestation, both the number of labelled cells and the level of *ARX* expression slowly decreased (Table 1). In our adult case, it was only expressed in a few cells such as neurons of layers I, II and IV of the cerebral cortex, as previously observed for cortical interneurons (Xu et al., 2011) and in the caudate nucleus, arguing for a role of ARX in mature neuron functioning of these structures. We then used MRI to investigate the consequences for adult patients of a defect in the function of this gene during brain development.

4.2. Brain anatomical structure changes in ARX patients

As we recently described a recognizable phenotype with a specific motor impairment in *ARX* dup24 patients (Curie et al., 2014), we decided to further characterize potential neuro-anatomical distinctive patterns associated with this mutation using high quality morphometric MRI data analyzed with FreeSurfer software. This automated procedure has already been validated using both neuropathology approaches performed on human post-mortem brain (Rosas et al., 2002), and manual measurements on human brain MRI (Salat et al., 2004). We show here that *ARX* patients have a significantly decreased striatal volume especially the caudate nuclei, and to a lesser extent of the thalamic and sub-thalamic nuclei, associated to a decrease in cortical thickness of the precentral gyrus and hippocampus. Interestingly, the implication of basal ganglia in the pathophysiology of ARX-related phenotypes has already been suggested in the literature. Histopathological studies on XLAG (X-linked Lissencephaly with Abnormal Genitalia) human patients have revealed poorly delineated and atrophic basal ganglia with small fragmented caudate nuclei (Bonneau et al., 2002). Moreover, Colombo et al. have reported functional impairment of the basal ganglia morphogenesis in *Arx* knock-out mice (Colombo et al., 2007). It is therefore conceivable that *ARX* dup24 mutation responsible for a partial loss-of-function can lead to subtle defects in the development and differentiation of basal ganglia, which may be visible only by using high quality morphometric MRI technology.

This hypothesis is further reinforced by the fact that basal ganglia are known to regulate sensorimotor processing and are especially involved in precision grip force control (Prodoehl et al., 2009; Wasson et al., 2010), a function that is altered in *ARX* dup24 patients who

present a very peculiar impairment of upper limb distal motor function with a pathognomonic hand-grip, similarly to the distortion of individual finger movements and posture observed in LKA. This particular "reach and grip" was not found in a group of age- and IQ-matched Down Syndrome (DS) patients who served as controls to ensure this was not related to low-cognitive functioning (Curie et al., 2014). Precision grip control requires precise and fine manipulation of the forces applied to the object being gripped (Prodoehl et al., 2009). During a gripping task, the following brain regions are active: primary sensorimotor cortex, dorsolateral premotor cortex, cerebellum and basal ganglia. The motor cortex and the basal ganglia allow the programming, selection and execution of movements. They act in concert owing to the close connections between the two structures. Information coming from the premotor and motor cortices is transmitted to the basal ganglia, mainly the striatum, which selects and activates motor planning allowing the proper motor activity and inhibits aberrant motor planning. In healthy controls, precision grip force tasks lead to increased activity in all basal ganglia (Prodoehl et al., 2009). Interestingly, an fMRI study showed that caudate nuclei are involved in selecting the amplitude of force contractions (Vaillancourt et al., 2007). Anterior nuclei in the basal ganglia such as caudate and anterior putamen are involved in the predictive scaling of precision grip force control (Wasson et al., 2010). Specific anterior nuclei of the basal ganglia are thus involved in planning aspects of precision grip force, whereas more posteriorly located nuclei (such as subthalamic nuclei and internal portion of the globus pallidus) are involved in dynamic parameters of grip force output (Vaillancourt et al., 2007; Prodoehl et al., 2009; Wasson et al., 2010). There are many movement disorders that arise as a result of basal ganglia dysfunction (Parkinson disease, dystonia, Huntington disease…) (Prodoehl et al., 2009; Spraker et al., 2010).

DS patients have been shown to have relatively preserved basal ganglia which appear to be enlarged by comparison with the overall cerebral brain reduction in DS patients (Pinter et al., 2001; White et al., 2003; Schaer and Eliez, 2007). This suggests that the combined decrease in cortical thickness of the primary motor cortex and basal ganglia volume we identified in *ARX* dup 24 patients may be considered as a hallmark of the disease and is likely to be the substrate of their specific motor phenotype. The smaller the caudate was, the thinner the precentral cortical thickness was. This hypothesis is further strengthened by the significant correlation observed between the volume of the caudate nucleus and the degree of motor impairment quantified by kinematic parameters of the precision grip in *ARX* patients. In the most severe forms associated with *ARX* dup24 mutation (Partington syndrome) major hand dystonia was observed, but mild to moderate focal dystonia (while holding a pen) was observed in 74% of the *ARX* patients (Curie et al., 2014). It is interesting to note that dystonia is not related to the dysfunction of one single brain region, but rather involves a motor network including basal ganglia, cerebellum, thalamus and sensorimotor cortex (Jinnah et al., 2017). We can probably here exclude cerebellum as we did not find any difference in cerebellum volume comparing *ARX* patients to age- and sex-matched healthy controls, an observation which is consistent with the absence of *ARX* expression in the developing and adult cerebellum. But we did find changes in the other nodes of this motor network. It would also be very interesting to study the structural and functional connectivity between these nodes (Mohammadi et al., 2012; Jinnah et al., 2017; Mantel et al., 2018).

In addition to the significant decrease observed in striatal volume, we also observed a decrease of thalamic and sub-thalamic nuclei volumes. Nevertheless, we did not find any relationship between the decreased thalamic volume and motor impairment. Importantly, the GE has been shown to contribute neurons to the thalamic nuclei in humans (Letinic and Kostovic, 1997; Letinic and Rakic, 2001). These cells migrate through the gangliothalamic body, a unique transient structure observed only in humans and present from 15 to 34 WG, followed by a progressive decrease from 34 WG. Phylogenetically, it is striking to note that this neuronal migrating pattern is unique to human. It has not been found in any other species including monkeys, in which all cells of dorsal thalamus come exclusively from the diencephalon. The gangliothalamic body is a stream of migrating bipolar neurons which rely on homotypic-neurophilic guidance, eventually form GABAergic neurons in the pulvinar and in the dorsal as well as mediodorsal subnuclei of the thalamus, which are anatomically related to both primary and associative cortical areas involved in higher cognitive functions, including symbolic reasoning or language (Letinic and Rakic, 2001). It is interesting to note that a thalamus volume decrease has been found in other X-linked ID such as *Rab-GDI* mutated patients (Curie et al., 2009), suggesting that this distinctive feature could also contribute to ID. On the contrary, increased thalamic volume has been reported in Fragile X syndrome patients (Reiss et al., 1995; Eliez et al., 2001; Gothelf et al., 2008), showing that the relationship between thalamus volume and ID remains unclear but it could offer new avenues to be explored. Recently, Sunnen et al. reported that *Arx* knock-out mice lost expression of specific markers of the thalamic reticular nucleus, which is entirely composed of GABAergic neurons, and of the zona incerta, an important pathway to the reticular nucleus of the thalamus, confirming a role of ARX in the development of these thalamic subnuclei (Sunnen et al., 2014).

We also observed an association between the Vineland Adaptive Behavior scale in *ARX* patients and their cortical thickness. The thinner the prefrontal cortex was, the more impaired the Vineland Adaptive Behavior scale was. It has been shown in typically developing children and adolescents that the profile of prefrontal cortical thickness maturation is closely related to the level of intelligence (Shaw et al., 2006) and that the activation of the prefrontal cortex during task correlates with intelligence in healthy subjects (Duncan et al., 2000; Gray et al., 2003). Moreover, Fragile X syndrome patients have decreased frontal lobe volume (Hallahan et al., 2011), aberrant maturation of the prefrontal cortex during adolescence (Bray et al., 2011) and atypical fronto-striatal circuitry (Barnea-Goraly et al., 2003; Haas et al., 2009), all associated with their executive functioning deficit (Fung et al., 2012). It has been suggested that ID patients could have a specific impairment in executive functioning (Danielsson et al., 2010; Danielsson et al., 2012). We recently showed that *ARX* patients were more impaired by inhibition (one main component of executive functioning) than their respective mental-age matched healthy controls in a visual analogical reasoning task (Curie et al., 2016). Our data are in concordance with this hypothesis, as the prefrontal cortex thinning is associated with weaker adaptive skills in *ARX* patients, reflecting the level of ID. Furthermore, in addition to the role in motor processes, basa ganglia have recently been shown to be also involved in cognitive (working memory, and executive functions), and affective (emotion and reward) processes (Arsalidou et al., 2013). Interestingly, we found a correlation between the prefrontal cortical thinning and the caudate volume: the thinner the prefrontal cortical thickness was, the smaller the caudate was. It is possible that the basal ganglia alteration in ARX patients contributes to their cognitive phenotype.

5. Conclusion

This study is the first to describe ARX expression in human brain at different developmental stages and the consequences of *ARX* dup24 mutation in human using quantitative MRI *in vivo*. It demonstrates that MRI is a powerful tool for the study of neuroanatomical profiles in rare diseases with ID. It would be very interesting in the future to replicate this structural study on a larger population of patients and at higher magnetic field, and to add functional MRI acquisition to better characterize the spatial and temporal patterns of brain activity in this patient population. Taken together, our findings confirm the key role of ARX in the generation, migration and function of GABAergic neurons both in the cerebral cortex, the basal ganglia and thalamus, providing some insights to explain the peculiar motor phenotype observed in *ARX* dup24 patients. It would be very interesting to further characterize the

corticobasal networks structural connectivity by using diffusion MRI.

Aknowledgements

Authors are indebted to patients and their families and caregivers. Special thanks for the support of the French XLMR parents' association “Xtraordinaire”.

Funding sources

Financial support was provided from the French Ministry of Health (PHRC grant 2010-A00327-32, VDP), the CNRS/Hospices Civils de Lyon (research fellow postgraduate grant for AC), the Foundation Jérôme Lejeune (grants for AC and GF, 2013), the “Xtraordinaire” association (grant for AC 2015), the ARRENNE association (grant for AC, 2012 and 2014) and IBSAM (grant for GF, 2017).

The authors declare that they have no conflicts of interest.

Appendix A. Supplementary data

Supplementary data to this article can be found online at https://doi.org/10.1016/j.nicl.2018.04.001.

References

Arsalidou, M., Duerden, E.G., Taylor, M.J., 2013. The centre of the brain: topographical model of motor, cognitive, affective, and somatosensory functions of the basal ganglia. Hum. Brain Mapp. 34 (11), 3031–3054.

Barnea-Goraly, N., Eliez, S., Hedeus, M., Menon, V., White, C.D., Moseley, M., Reiss, A.L., 2003. White matter tract alterations in fragile X syndrome: preliminary evidence from diffusion tensor imaging. Am. J. Med. Genet. B Neuropsychiatr. Genet. 118B (1), 81–88.

Bayer, S.A., Altman, J., 2004. Atlas of Human Central Nervous System Development, Vol 2 and 3: The Human Brain during the Second and Third Trimester. CRC Press, Boca Raton, FL.

Beguin, S., Crepel, V., Aniksztejn, L., Becq, H., Pelosi, B., Pallesi-Pocachard, E., Bouamrane, L., Pasqualetti, M., Kitamura, K., Cardoso, C., Represa, A., 2013. An epilepsy-related ARX polyalanine expansion modifies glutamatergic neurons excitability and morphology without affecting GABAergic neurons development. Cereb. Cortex 23 (6), 1484–1494.

Bienvenu, T., Poirier, K., Friocourt, G., Bahi, N., Beaumont, D., Fauchereau, F., Ben Jeema, L., Zemni, R., Vinet, M.C., Francis, F., Couvert, P., Gomot, M., Moraine, C., van Bokhoven, H., Kalscheuer, V., Frints, S., Gecz, J., Ohzaki, K., Chaabouni, H., Fryns, J.P., Desportes, V., Beldjord, C., Chelly, J., 2002. ARX, a novel Prd-class-homeobox gene highly expressed in the telencephalon, is mutated in X-linked mental retardation. Hum. Mol. Genet. 11 (8), 981–991.

Biressi, S., Messina, G., Collombat, P., Tagliafico, E., Monteverde, S., Benedetti, L., Cusella De Angelis, M.G., Mansouri, A., Ferrari, S., Tajbakhsh, S., Broccoli, V., Cossu, G., 2008. The homeobox gene Arx is a novel positive regulator of embryonic myogenesis. Cell Death Differ. 15 (1), 94–104.

Bonneau, D., Toutain, A., Laquerriere, A., Marret, S., Saugier-Veber, P., Barthez, M.A., Radi, S., Biran-Mucignat, V., Rodriguez, D., Gelot, A., 2002. X-linked lissencephaly with absent corpus callosum and ambiguous genitalia (XLAG): clinical, magnetic resonance imaging, and neuropathological findings. Ann. Neurol. 51 (3), 340–349.

Bray, S., Hirt, M., Jo, B., Hall, S.S., Lightbody, A.A., Walter, E., Chen, K., Patnaik, S., Reiss, A.L., 2011. Aberrant frontal lobe maturation in adolescents with fragile X syndrome is related to delayed cognitive maturation. Biol. Psychiatry 70 (9), 852–858.

Clowry, G.J., 2015. An enhanced role and expanded developmental origins for gamma-aminobutyric acidergic interneurons in the human cerebral cortex. J. Anat. 227 (4), 384–393.

Cobos, I., Broccoli, V., Rubenstein, J.L., 2005. The vertebrate ortholog of Aristaless is regulated by Dlx genes in the developing forebrain. J. Comp. Neurol. 483 (3), 292–303.

Colasante, G., Simonet, J.C., Calogero, R., Crispi, S., Sessa, A., Cho, G., Golden, J.A., Broccoli, V., 2015. ARX regulates cortical intermediate progenitor cell expansion and upper layer neuron formation through repression of Cdkn1c. Cereb. Cortex 25 (2), 322–335.

Collombat, P., Mansouri, A., Hecksher-Sorensen, J., Serup, P., Krull, J., Gradwohl, G., Gruss, P., 2003. Opposing actions of Arx and Pax4 in endocrine pancreas development. Genes Dev. 17 (20), 2591–2603.

Colombo, E., Galli, R., Cossu, G., Gecz, J., Broccoli, V., 2004. Mouse orthologue of ARX, a gene mutated in several X-linked forms of mental retardation and epilepsy, is a marker of adult neural stem cells and forebrain GABAergic neurons. Dev. Dyn. 231 (3), 631–639.

Colombo, E., Collombat, P., Colasante, G., Bianchi, M., Long, J., Mansouri, A., Rubenstein, J.L., Broccoli, V., 2007. Inactivation of Arx, the murine ortholog of the X-linked lissencephaly with ambiguous genitalia gene, leads to severe disorganization of the ventral telencephalon with impaired neuronal migration and differentiation. J. Neurosci. 27 (17), 4786–4798.

Corbin, J.G., Nery, S., Fishell, G., 2001. Telencephalic cells take a tangent: non-radial migration in the mammalian forebrain. Nat. Neurosci. 4 (Suppl), 1177–1182.

Curie, A., Sacco, S., Bussy, G., de Saint Martin, A., Boddaert, N., Chanraud, S., Meresse, I., Chelly, J., Zilbovicius, M., Portes, V. des, 2009. Impairment of cerebello-thalamo-frontal pathway in Rab-GDI mutated patients with pure mental deficiency. Eur. J. Med. Genet. 52 (1), 6–13.

Curie, A., Nazir, T., Brun, A., Paulignan, Y., Reboul, A., Delange, K., Cheylus, A., Bertrand, S., Rochefort, F., Bussy, G., Marignier, S., Lacombe, D., Chiron, C., Cossee, M., Leheup, B., Philippe, C., Laugel, V., De Saint Martin, A., Sacco, S., Poirier, K., Bienvenu, T., Souville, I., Gilbert-Dussardier, B., Bieth, E., Kauffmann, D., Briot, P., de Freminville, B., Prieur, F., Till, M., Rooryck-Thambo, C., Mortemousque, I., Bobillier-Chaumont, I., Toutain, A., Touraine, R., Sanlaville, D., Chelly, J., Freeman, S., Kong, J., Hadjikhani, N., Gollub, R.L., Roy, A., des Portes, V., 2014. The c.429_452 duplication of the ARX gene: a unique developmental-model of limb kinetic apraxia. Orphanet J. Rare Dis. 9, 25.

Curie, A., Brun, A., Cheylus, A., Reboul, A., Nazir, T., Bussy, G., Delange, K., Paulignan, Y., Mercier, S., David, A., Marignier, S., Merle, L., de Freminville, B., Prieur, F., Till, M., Mortemousque, I., Toutain, A., Bieth, E., Touraine, R., Sanlaville, D., Chelly, J., Kong, J., Ott, D., Kassai, B., Hadjikhani, N., Gollub, R.L., des Portes, V., 2016. A novel analog reasoning paradigm: new insights in intellectually disabled patients. PLoS One 11 (2), e0149717.

Dale, A.M., Fischl, B., Sereno, M.I., 1999. Cortical surface-based analysis. I. Segmentation and surface reconstruction. NeuroImage 9 (2), 179–194.

Danielsson, H., Henry, L., Ronnberg, J., Nilsson, L.G., 2010. Executive functions in individuals with intellectual disability. Res. Dev. Disabil. 31 (6), 1299–1304.

Danielsson, H., Henry, L., Messer, D., Ronnberg, J., 2012. Strengths and weaknesses in executive functioning in children with intellectual disability. Res. Dev. Disabil. 33 (2), 600–607.

Duncan, J., Seitz, R.J., Kolodny, J., Bor, D., Herzog, H., Ahmed, A., Newell, F.N., Emslie, H., 2000. A neural basis for general intelligence. Science 289 (5478), 457–460.

Eliez, S., Blasey, C.M., Freund, L.S., Hastie, T., Reiss, A.L., 2001. Brain anatomy, gender and IQ in children and adolescents with fragile X syndrome. Brain 124 (Pt 8), 1610–1618.

Feess-Higgins, A., Larroche, J.C., 1987. Le développement du cerveau foetal humain. In: Atlas Anatomique. INSERM-CNRS, Masson (éd.), Paris.

Fischl, B., Dale, A.M., 2000. Measuring the thickness of the human cerebral cortex from magnetic resonance images. Proc. Natl. Acad. Sci. U. S. A. 97 (20), 11050–11055.

Fischl, B., Sereno, M.I., Dale, A.M., 1999. Cortical surface-based analysis. II: inflation, flattening, and a surface-based coordinate system. NeuroImage 9 (2), 195–207.

Fischl, B., Liu, A., Dale, A.M., 2001. Automated manifold surgery: constructing geometrically accurate and topologically correct models of the human cerebral cortex. IEEE Trans. Med. Imaging 20 (1), 70–80.

Fischl, B., Salat, D.H., Busa, E., Albert, M., Dieterich, M., Haselgrove, C., van der Kouwe, A., Killiany, R., Kennedy, D., Klaveness, S., Montillo, A., Makris, N., Rosen, B., Dale, A.M., 2002. Whole brain segmentation: automated labeling of neuroanatomical structures in the human brain. Neuron 33 (3), 341–355.

Friocourt, G., Parnavelas, J.G., 2010. Mutations in ARX result in several defects involving GABAergic neurons. Front. Cell. Neurosci. 4, 4.

Friocourt, G., Poirier, K., Rakic, S., Parnavelas, J.G., Chelly, J., 2006. The role of ARX in cortical development. Eur. J. Neurosci. 23 (4), 869–876.

Friocourt, G., Kanatani, S., Tabata, H., Yozu, M., Takahashi, T., Antypa, M., Raguenes, O., Chelly, J., Ferec, C., Nakajima, K., Parnavelas, J.G., 2008. Cell-autonomous roles of ARX in cell proliferation and neuronal migration during corticogenesis. J. Neurosci. 28 (22), 5794–5805.

Fung, L.K., Quintin, E.M., Haas, B.W., Reiss, A.L., 2012. Conceptualizing neurodevelopmental disorders through a mechanistic understanding of fragile X syndrome and Williams syndrome. Curr. Opin. Neurol. 25 (2), 112–124.

Gothelf, D., Furfaro, J.A., Hoeft, F., Eckert, M.A., Hall, S.S., O'Hara, R., Erba, H.W., Ringel, J., Hayashi, K.M., Patnaik, S., Golianu, B., Kraemer, H.C., Thompson, P.M., Piven, J., Reiss, A.L., 2008. Neuroanatomy of fragile X syndrome is associated with aberrant behavior and the fragile X mental retardation protein (FMRP). Ann. Neurol. 63 (1), 40–51.

Gray, J.R., Chabris, C.F., Braver, T.S., 2003. Neural mechanisms of general fluid intelligence. Nat. Neurosci. 6 (3), 316–322.

Guihard-Costa, A.M., Larroche, J.C., 1990. Differential growth between the fetal brain and its infratentorial part. Early Hum. Dev. 23 (1), 27–40.

Haas, B.W., Barnea-Goraly, N., Lightbody, A.A., Patnaik, S.S., Hoeft, F., Hazlett, H., Piven, J., Reiss, A.L., 2009. Early white-matter abnormalities of the ventral frontostriatal pathway in fragile X syndrome. Dev. Med. Child Neurol. 51 (8), 593–599.

Hallahan, B.P., Craig, M.C., Toal, F., Daly, E.M., Moore, C.J., Ambikapathy, A., Robertson, D., Murphy, K.C., Murphy, D.G., 2011. In vivo brain anatomy of adult males with fragile X syndrome: an MRI study. NeuroImage 54 (1), 16–24.

Han, X., Jovicich, J., Salat, D., van der Kouwe, A., Quinn, B., Czanner, S., Busa, E., Pacheco, J., Albert, M., Killiany, R., Maguire, P., Rosas, D., Makris, N., Dale, A., Dickerson, B., Fischl, B., 2006. Reliability of MRI-derived measurements of human cerebral cortical thickness: the effects of field strength, scanner upgrade and manufacturer. NeuroImage 32 (1), 180–194.

Hansen, D.V., Lui, J.H., Flandin, P., Yoshikawa, K., Rubenstein, J.L., Alvarez-Buylla, A., Kriegstein, A.R., 2013. Non-epithelial stem cells and cortical interneuron production in the human ganglionic eminences. Nat. Neurosci. 16 (11), 1576–1587.

Jinnah, H.A., Neychev, V., Hess, E.J., 2017. The anatomical basis for dystonia: the motor network model. Tremor Other Hyperkinet. Mov. 7, 506.

Kato, M., Dobyns, W.B., 2005. X-linked lissencephaly with abnormal genitalia as a tangential migration disorder causing intractable epilepsy: proposal for a new term, “interneuronopathy”. J. Child Neurol. 20 (4), 392–397.

Kitamura, K., Yanazawa, M., Sugiyama, N., Miura, H., Iizuka-Kogo, A., Kusaka, M., Omichi, K., Suzuki, R., Kato-Fukui, Y., Kamiirisa, K., Matsuo, M., Kamijo, S., Kasahara, M., Yoshioka, H., Ogata, T., Fukuda, T., Kondo, I., Kato, M., Dobyns, W.B., Yokoyama, M., Morohashi, K., 2002. Mutation of ARX causes abnormal development of forebrain and testes in mice and X-linked lissencephaly with abnormal genitalia in humans. Nat. Genet. 32 (3), 359–369.

Lee, K., Mattiske, T., Kitamura, K., Gecz, J., Shoubridge, C., 2014. Reduced polyalanine-expanded Arx mutant protein in developing mouse subpallium alters Lmo1 transcriptional regulation. Hum. Mol. Genet. 23 (4), 1084–1094.

Letinic, K., Kostovic, I., 1997. Transient fetal structure, the gangliothalamic body, connects telencephalic germinal zone with all thalamic regions in the developing human brain. J. Comp. Neurol. 384 (3), 373–395.

Letinic, K., Rakic, P., 2001. Telencephalic origin of human thalamic GABAergic neurons. Nat. Neurosci. 4 (9), 931–936.

Mantel, T., Meindl, T., Li, Y., Jochim, A., Gora-Stahlberg, G., Kraenbring, J., Berndt, M., Dresel, C., Haslinger, B., 2018. Network-specific resting-state connectivity changes in the premotor-parietal axis in writer's cramp. Neuroimage Clin. 17, 137–144.

Marcorelles, P., Laquerriere, A., Adde-Michel, C., Marret, S., Saugier-Veber, P., Beldjord, C., Friocourt, G., 2010. Evidence for tangential migration disturbances in human lissencephaly resulting from a defect in LIS1, DCX and ARX genes. Acta Neuropathol. 120 (4), 503–515.

Marin, O., Anderson, S.A., Rubenstein, J.L., 2000. Origin and molecular specification of striatal interneurons. J. Neurosci. 20 (16), 6063–6076.

Miura, H., Yanazawa, M., Kato, K., Kitamura, K., 1997. Expression of a novel aristaless related homeobox gene 'Arx' in the vertebrate telencephalon, diencephalon and floor plate. Mech. Dev. 65 (1–2), 99–109.

Mohammadi, B., Kollewe, K., Samii, A., Beckmann, C.F., Dengler, R., Munte, T.F., 2012. Changes in resting-state brain networks in writer's cramp. Hum. Brain Mapp. 33 (4), 840–848.

Nobrega-Pereira, S., Gelman, D., Bartolini, G., Pla, R., Pierani, A., Marin, O., 2010. Origin and molecular specification of globus pallidus neurons. J. Neurosci. 30 (8), 2824–2834.

O'Brien, L.M., Ziegler, D.A., Deutsch, C.K., Frazier, J.A., Herbert, M.R., Locascio, J.J., 2011. Statistical adjustments for brain size in volumetric neuroimaging studies: some practical implications in methods. Psychiatry Res. 193 (2), 113–122.

Olivetti, P.R., Noebels, J.L., 2012. Interneuron, interrupted: molecular pathogenesis of ARX mutations and X-linked infantile spasms. Curr. Opin. Neurobiol. 22 (5), 859–865.

Parnavelas, J.G., 2000. The origin and migration of cortical neurones: new vistas. Trends Neurosci. 23 (3), 126–131.

Pinter, J.D., Eliez, S., Schmitt, J.E., Capone, G.T., Reiss, A.L., 2001. Neuroanatomy of Down's syndrome: a high-resolution MRI study. Am. J. Psychiatry 158 (10), 1659–1665.

Poirier, K., Van Esch, H., Friocourt, G., Saillour, Y., Bahi, N., Backer, S., Souil, E., Castelnau-Ptakhine, L., Beldjord, C., Francis, F., Bienvenu, T., Chelly, J., 2004. Neuroanatomical distribution of ARX in brain and its localisation in GABAergic neurons. Brain Res. Mol. Brain Res. 122 (1), 35–46.

Poirier, K., Lacombe, D., Gilbert-Dussardier, B., Raynaud, M., Desportes, V., de Brouwer, A.P., Moraine, C., Fryns, J.P., Ropers, H.H., Beldjord, C., Chelly, J., Bienvenu, T., 2006. Screening of ARX in mental retardation families: consequences for the strategy of molecular diagnosis. Neurogenetics 7 (1), 39–46.

Pombero, A., Bueno, C., Saglietti, L., Rodenas, M., Guimera, J., Bulfone, A., Martinez, S., 2011. Pallial origin of basal forebrain cholinergic neurons in the nucleus basalis of Meynert and horizontal limb of the diagonal band nucleus. Development 138 (19), 4315–4326.

Price, M.G., Yoo, J.W., Burgess, D.L., Deng, F., Hrachovy, R.A., Frost Jr., J.D., Noebels, J.L., 2009. A triplet repeat expansion genetic mouse model of infantile spasms syndrome, Arx(GCG)10 + 7, with interneuronopathy, spasms in infancy, persistent seizures, and adult cognitive and behavioral impairment. J. Neurosci. 29 (27), 8752–8763.

Prodoehl, J., Corcos, D.M., Vaillancourt, D.E., 2009. Basal ganglia mechanisms underlying precision grip force control. Neurosci. Biobehav. Rev. 33 (6), 900–908.

Rakic, P., 2009. Evolution of the neocortex: a perspective from developmental biology. Nat. Rev. Neurosci. 10 (10), 724–735.

Reiss, A.L., Abrams, M.T., Greenlaw, R., Freund, L., Denckla, M.B., 1995. Neurodevelopmental effects of the FMR-1 full mutation in humans. Nat. Med. 1 (2), 159–167.

Rosas, H.D., Liu, A.K., Hersch, S., Glessner, M., Ferrante, R.J., Salat, D.H., van der Kouwe, A., Jenkins, B.G., Dale, A.M., Fischl, B., 2002. Regional and progressive thinning of the cortical ribbon in Huntington's disease. Neurology 58 (5), 695–701.

Salat, D.H., Buckner, R.L., Snyder, A.Z., Greve, D.N., Desikan, R.S., Busa, E., Morris, J.C., Dale, A.M., Fischl, B., 2004. Thinning of the cerebral cortex in aging. Cereb. Cortex 14 (7), 721–730.

Schaer, M., Eliez, S., 2007. From genes to brain: understanding brain development in neurogenetic disorders using neuroimaging techniques. Child Adolesc. Psychiatr. Clin. N. Am. 16 (3), 557–579.

Segonne, F., Pacheco, J., Fischl, B., 2007. Geometrically accurate topology-correction of cortical surfaces using nonseparating loops. IEEE Trans. Med. Imaging 26, 518–529.

Shaw, P., Greenstein, D., Lerch, J., Clasen, L., Lenroot, R., Gogtay, N., Evans, A., Rapoport, J., Giedd, J., 2006. Intellectual ability and cortical development in children and adolescents. Nature 440 (7084), 676–679.

Shoubridge, C., Fullston, T., Gecz, J., 2010. ARX spectrum disorders: making inroads into the molecular pathology. Hum. Mutat. 31 (8), 889–900.

Simonet, J.C., Sunnen, C.N., Wu, J., Golden, J.A., Marsh, E.D., 2015. Conditional loss of Arx from the developing dorsal telencephalon results in behavioral phenotypes resembling mild human ARX mutations. Cereb. Cortex 25 (9), 2939–2950.

Spraker, M.B., Prodoehl, J., Corcos, D.M., Comella, C.L., Vaillancourt, D.E., 2010. Basal ganglia hypoactivity during grip force in drug naive Parkinson's disease. Hum. Brain Mapp. 31 (12), 1928–1941.

Sunnen, C.N., Simonet, J.C., Marsh, E.D., Golden, J.A., 2014. Arx is required for specification of the zona incerta and reticular nucleus of the thalamus. J. Neuropathol. Exp. Neurol. 73 (3), 253–261.

Vaillancourt, D.E., Yu, H., Mayka, M.A., Corcos, D.M., 2007. Role of the basal ganglia and frontal cortex in selecting and producing internally guided force pulses. NeuroImage 36 (3), 793–803.

Wasson, P., Prodoehl, J., Coombes, S.A., Corcos, D.M., Vaillancourt, D.E., 2010. Predicting grip force amplitude involves circuits in the anterior basal ganglia. NeuroImage 49 (4), 3230–3238.

White, N.S., Alkire, M.T., Haier, R.J., 2003. A voxel-based morphometric study of nondemented adults with down syndrome. NeuroImage 20 (1), 393–403.

Xu, G., Broadbelt, K.G., Haynes, R.L., Folkerth, R.D., Borenstein, N.S., Belliveau, R.A., Trachtenberg, F.L., Volpe, J.J., Kinney, H.C., 2011. Late development of the GABAergic system in the human cerebral cortex and white matter. J. Neuropathol. Exp. Neurol. 70 (10), 841–858.